Transport through Amorphous Photonic Materials with Localization and Bandgap Regimes

Frank Scheffold,[1,*] Jakub Haberko,[2] Sofia Magkiriadou,[1] and Luis S. Froufe-Pérez[1]
[1]Department of Physics, University of Fribourg, CH-1700 Fribourg, Switzerland
[2]Faculty of Physics and Applied Computer Science, AGH University of Science and Technology, Aleja Mickiewicza 30, Krakow 30-059, Poland

(Received 11 February 2022; accepted 30 August 2022; published 3 October 2022)

We propose a framework that unifies the description of light transmission through three-dimensional amorphous dielectric materials that exhibit both localization and a photonic bandgap. We argue that direct, coherent reflection near and in the bandgap attenuates the generation of diffuse or localized photons. Using the self-consistent theory of localization and considering the density of states of photons, we can quantitatively describe the total transmission of light for all transport regimes: transparency, light diffusion, localization, and bandgap. Comparison with numerical simulations of light transport through hyperuniform networks supports our theoretical approach.

DOI: 10.1103/PhysRevLett.129.157402

Photonic bandgaps (PBGs) and light localization fundamentally alter a dielectric material's wave transport properties [1,2]. In 1987, Yablonovitch proposed that crystal lattices composed of high and low index dielectric materials can lead to forbidden propagation in certain electromagnetic frequency bands [3]. More recently, researchers also demonstrated the existence of bandgaps in two- and three-dimensional disordered, amorphous dielectrics based on numerical simulations and experiments [4–10]. In particular, disordered "hyperuniform" photonic materials raised a lot of attention [11]. Several groups showed that these materials could exhibit isotropic complete photonic bandgaps nearly as wide as the corresponding crystal structure [4–6]. Bandgaps in amorphous dielectrics have renewed interest in strong Anderson localization (SAL) of light and other transport regimes in those materials. We, with others, proposed a transport phase diagram to organize numerical and experimental data [12–14]. However, recent three-dimensional finite-difference time-domain (FDTD) simulations have also shown that existing theoretical models cannot describe the transition between the localization and bandgap regimes [15], calling for a new and improved theoretical approach. In this Letter, we introduce a theoretical model based on the self-consistent theory of localization (SC theory) of a semi-infinite medium [16–18], together with an exponential direct reflection coefficient. We show that our model is capable of describing the transmission of light through amorphous photonic materials over the entire range of frequencies, encompassing all transport regimes.

Ballistic and diffuse transport of light.—The transmission of light through nonabsorbing disordered dielectrics is usually described by single scattering and multiple scattering, which turns into photon diffusion for many scattering events. For a wide slab, thickness L, the total transmission coefficient $T(L)$ is given by a ballistic contribution, $T_b(L) = e^{-L/\ell}$ with a scattering mean free path ℓ, a diffusive part $T_d(L)$ set by the transport mean free path ℓ^* and a crossover term considering the conversion of incident photons to diffusive photons via multiple scattering [19,20]. For optically dense samples ($L \gg \ell^*$), neglecting surface reflectivity, the diffusive total transmission coefficient is

$$T_d(L) \simeq \frac{1+z_0}{2z_0 + L/\ell^*} \overset{L\gg\ell^*}{\rightarrow} (1+z_0)\frac{\ell^*}{L}, \tag{1}$$

where z_0 is the extrapolation length ratio, a constant of order unity [19–22]. The scattering length ℓ and the transport mean free path ℓ^* are linked by the scattering anisotropy parameter $g = <\cos\Theta>_{d\sigma/d\Omega}$ with $\ell^*/\ell = 1/(1-g)$. For very small scatterers, or for the case of stealthy hyperuniformity, the differential scattering cross section becomes zero, $d\sigma/d\Omega, \ell^{-1} \equiv 0$, resulting in transparency with $T = 1$ independent of L [13,23,24].

Anderson localization of light.—Strong Anderson localization is an interference effect in multiple scattering of waves leading to exponentially attenuated diffuse transmission. SC theory describes SAL by introducing a position-dependent light diffusion coefficient $D(z)$, where z denotes the distance from the surface of a wide slab [16,17,25]. One needs to solve an implicit equation that contains the average return probability which is increased in the presence of SAL and, in turn, reduces $D(z)$ from

 © 2022 American Physical Society

$D(0)$ at the interface to zero deep inside the medium [17,18]. To this end, we replace L/ℓ^* in Eq. (1) and write

$$\frac{L}{\ell^*} \to \frac{\tilde{L}}{\ell^*} = \frac{1}{\ell^*}\int_0^L \frac{D_B}{D(z)}dz, \tag{2}$$

where $D_B = v_E\ell^*/3$ denotes the (Boltzmann) light diffusion coefficient for a speed of light v_E. Far from the localization regime $D(z) \equiv D_B$ and $\tilde{L} \equiv L$ [19,20,26]. For localization in a semi-infinite medium the SC theory solution is $D_\infty(z) \simeq D(0)e^{-2z/\xi}$, where ξ denotes the localization length. By interpolation, for a slab of finite thickness van Tiggelen *et al.* proposed $D(z) \simeq D_\infty(L/2 - |L/2 - z|)$ [17,18]. Because of the mirror symmetry relative to the center of the slab at $z = L/2$, we can take the integral in Eq. (2) from $z \in [0, L/2]$, $\tilde{L} = 2\int_0^{L/2}(D_B/D(0))e^{2z/\xi}dz$ and find

$$\frac{T_d(L)}{(1+z_0)} = \frac{1}{2z_0 + \frac{\xi D_B}{\ell^* D(0)}(e^{L/\xi} - 1)} \overset{L\gg\xi}{\to} \frac{\ell^* D(0)}{\xi D_B}e^{-L/\xi}. \tag{3}$$

At the localization transition ("mobility edge"), the full SC theory, for a finite thickness L, predicts a critical power-law decay $T_d \sim 1/L^2$, instead of an exponential [18]. The onset of this power law is captured by Eq. (3), which can be seen by expanding $e^{L/\xi} - 1 = L/\xi + (L/\xi)^2/2 + (L/\xi)^3/6\ldots$, but for thick slabs, $L/\xi \gtrsim 3$, it deviates. In numerical simulations of real world materials, the system sizes are limited, and a study of the critical regime is beyond the scope of the present Letter.

Direct coherent reflection.—Previous studies argued that the transmission probability T ($L \gg \ell^*$) is independent of the single scattering angular distribution and only depends on the transport mean free path ℓ^*, as expressed by Eq. (1) [19–21]. More recent work, driven mainly by the renewed interest in structural coloration, showed the importance of explicitly adding a single scattering reflection term in the presence of correlated disorder, for example, for photonic glasses [27–29]. Short range order in photonic glasses leads to coherent collective scattering that, for a matching wavelength, results in enhanced single scattering reflection. Compared to structural coloration, the opening of a gap in amorphous photonic materials provides an even stronger, coherent mechanism for direct reflection, fundamentally altering the way scattered photons convert into diffuse photons, Fig. 1. We follow the reasoning of Magkiriadou *et al.*, that the intensity of light directly reflected scales with $(\sigma_{\rm dr}/\sigma)e^{-z/\ell}$, where $\sigma_{\rm dr}$ denotes the direct reflection cross section and σ the total scattering cross section. The direct reflection from layers close to the surface is higher and the reflected intensity from inside the sample decreases exponentially as the coherent beam attenuates [27]. Simultaneously, direct reflection reduces the probability density for the creation of diffuse photons within a distance

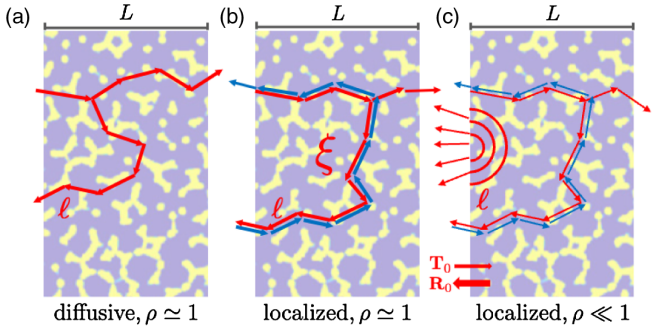

FIG. 1. Transport of light through amorphous hyperuniform silicon networks with localization and bandgap regimes. Lines indicate scattering paths. ℓ denotes the scattering mean free path. (a) Random multiple scattering and photon diffusion. (b) Loops of counter propagating paths signaling SAL with a localization length ξ are shown in red and blue color. (c) PBG regime with a small but finite density of states (DOS). The diffusive or SAL part $T_{\rm d}(L)$ is attenuated by a factor $T_0 = (1 - R_0)$ proportional to the normalized photonic DOS in the bulk $\rho(\nu')$. R_0 denotes the direct reflection factor. The background shows a cross section of the hyperuniform silicon network displayed in Fig. 2(a) with a slab thickness L.

z into the slab which now scales as $(1 - (\sigma_{\rm dr}/\sigma))e^{-z/\ell}$ [15,19]. For $\sigma_{\rm dr} = \sigma$, the reflection coefficient $R_0 = (\sigma_{\rm dr}/\sigma), = 1$, and all light is coherently reflected in the limit $L \gg \ell$. For $\sigma_{\rm dr} < \sigma$ a proportional amount $T_0 = 1 - R_0 = 1 - (\sigma_{\rm dr}/\sigma) < 1$ can couple to the diffuse up- and downstream of photons. Consequently, the total transmission coefficient is lowered to

$$T(L \gg \ell^*) = T_0 \times T_d(L). \tag{4}$$

We include an approximate expression for $T(L)$ covering the entire range of L in the Supplemental Material [30], Eq. (S1).

Numerical transport simulations.—To check the model predictions, Eq. (4), we performed FDTD simulations using the open source MIT Electromagnetic Equation Propagation (MEEP) package on a computer cluster [15,31]. We generate hyperuniform network structures, Fig. 2(a), using a custom-made code based on a 10 000-particle jammed seed pattern taken from Ref. [32], volume filling fraction ~0.64. Jammed, random close sphere packings display nearly hyperuniform behavior at large length scales [10,33]. All units are given relative to the diameter a of the spheres of the seed pattern. Next, we perform a Delaunay tessellation of the seed pattern. The tessellation divides the pattern into tetrahedra. We connect the centers of mass of the tetrahedra with dielectric rods, creating the desired tetravalent network structure [6,7]. We apply a silicon refractive index $n = 3.6$ and a volume filling fraction of $\phi = 0.28$. We cut the digital box into slices to obtain slabs of different thicknesses $L \leq 18a$, footprint $18a \times 18a$. In the MEEP simulation, we apply periodic

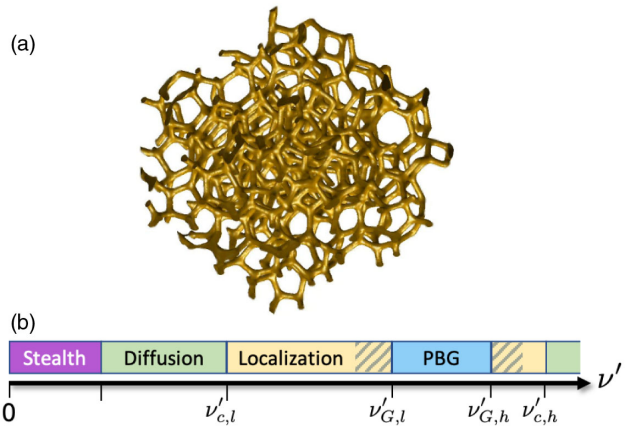

FIG. 2. (a) Rendering of a three-dimensional hyperuniform silicon network structure in air with a volume filling fraction of $\phi = 0.28$ derived from the center positions of randomly close-packed spheres, diameter a [15,38], which also sets the characteristic length scale of short-range spatial correlations [6,15]. The refractive index is $n = 3.6$ and the host medium is air, $n_{\text{air}} = 1$. (b) Transport phase diagram for electromagnetic waves in disordered photonic materials as a function of the dimensionless frequency $\nu' = a/\lambda = \nu \times a/v_E$, adapted from [12]. λ denotes the vacuum wavelength and v_E the speed of light. For low frequencies, stealthy hyperuniform materials show transparency. For weak or moderate scattering, light transport is "diffusive" followed by strong Anderson "localization" (SAL) with transitions at ν'_c and a bandgap regime ("PBG") around ν'_G. Closer to the gap the reduced density of states influences localization, shaded areas. The midgap frequency is $\nu'_G \sim 0.50$, in agreement with the Bragg condition in a corresponding crystal $\lambda = a/\nu' \sim 2a$ [15].

boundary conditions perpendicular to the propagation axis, and we add perfectly matched layers at both ends of the simulation box acting as absorbers. We send a pulse of linearly polarized light and record the Poynting vector on a monitor located behind the structure. The transmission coefficient $T(L, \nu')$ is defined as the ratio of the transmitted power to the incoming power. In total, we study twenty three sample thicknesses ranging from $L = 0.3$–$18a$, averaged over 6 (thick slabs) to 15 (thin slabs) samples [15,34].

In Fig. 3, we show the FDTD data for the total transmission $T(L)$ at different frequencies in the localization and bandgap regime. We fit the initial decay for $L \lesssim a$ with $T_b(L) = e^{-L/\ell}$ and extract the mean free path $\ell(\nu')$. Using this ballistic $\ell(\nu')$, we fit the data for thick slabs, $7a < L < 18a$ ($L \gg \ell$) using Eq. (4) with $z_0 = 3.25$ from Ref. [15]. For simplicity, we assume $\ell^* \sim \ell$ and $D_B/D(0) \simeq (1 + 2z_0/\xi)$ in the localized regime [18]. As shown in Fig. 3, we find excellent agreement between the fit and FDTD data. The attenuation of the incident beam by coherent reflection can become very strong, with $T_0 \to 0$, close to and in the PBG. From the fit to $T_d(L)$, we extract $\xi(\nu')$ and $T_0(\nu')$.

In Fig. 4, we plot the frequency dependence of all parameters obtained by the model fit. The mean free path, ℓ, and thus also $k\ell$, decay toward the bandgap is approached and reach a minimal value $k\ell = (2\pi\ell/\lambda) \sim 2$ ($\ell/a \sim 0.65$) in the bandgap center [15], Fig. 4(a). Approaching the gap, ξ/a drops, and the smallest value we observe is $\xi/a \gtrsim 3$; see, also, Fig. 3(c). van Tiggelen *et al.* proposed for the $k\ell$ dependence of the localization length $\xi \propto (k\ell)^2/\{1 - [k\ell/(k\ell)_c]^4\}$ [18,35,36]. Adjusting $(k\ell)_c$ values, we find a lower (l) and higher (h) frequency mobility edge $\nu'_{c,l} \simeq 0.37$ at $kl = (kl)_{c,l} = 4.1$ and at $\nu_c, h' \simeq 0.53$ for $kl = (kl)_{c,h} = 2.85$, Fig. 4(b). We only consider values $\xi/a < 18$ (smaller than the system size). The agreement between theory and data is remarkable. However, we find better agreement with the dimensionless ξ/a compared to the originally suggested ξ/ℓ. Moreover, the expression for ξ does not consider the DOS. In a recent dissertation [37], Monsarrat derives a slightly different formula for the localization length from SC theory that explicitly accounts for the DOS and does not scale with $k\ell^*$

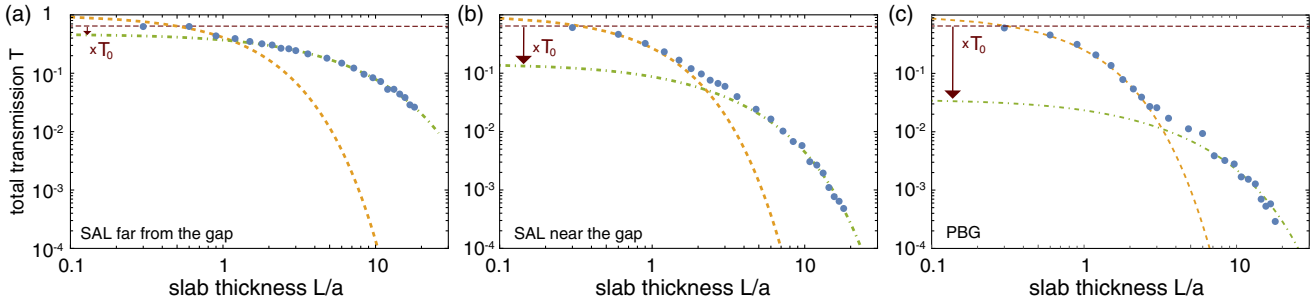

FIG. 3. Total transmission $T(L)$ as a function of the reduced slab thickness L/a in log-log representation for three different frequencies ν' in the localized and bandgap regime. Filled blue circles show the results from FDTD simulations averaged over 6 (thick slabs) to 15 (thin slabs) samples. The dashed orange line shows the fit with $T_b(L) = e^{-L/\ell}$ over $L \lesssim a$ which yields $\ell(\nu')$. The dash-dotted green line shows the fit with $T_0 \times T_d(L)$ over $7a < L < 18a$ which yields $\xi(\nu')$ and $T_0(\nu')$. (a) Localization: $\nu' = 0.418$, $\ell/a = 1.12, \xi/a = 8$, and $T_0 = 0.72 \sim 1$. (b) Localization near the PBG: $\nu' = 0.462$, $\ell/a = 0.76, \xi/a = 3.6$, and $T_0 = 0.22$, (c) Nearly complete PBG: $\nu' = 0.471$, $\ell/a = 0.72, \xi/a = 5.1$, and $T_0 = 0.055$. $z_0 = 3.25$, taken from [15]. Horizontal dashed line: $T_d(0) = (1 + z_0)/2z_0 = 0.65$, Eq. (1). Additional plots are shown in the Supplemental Material [30], Fig. S3.

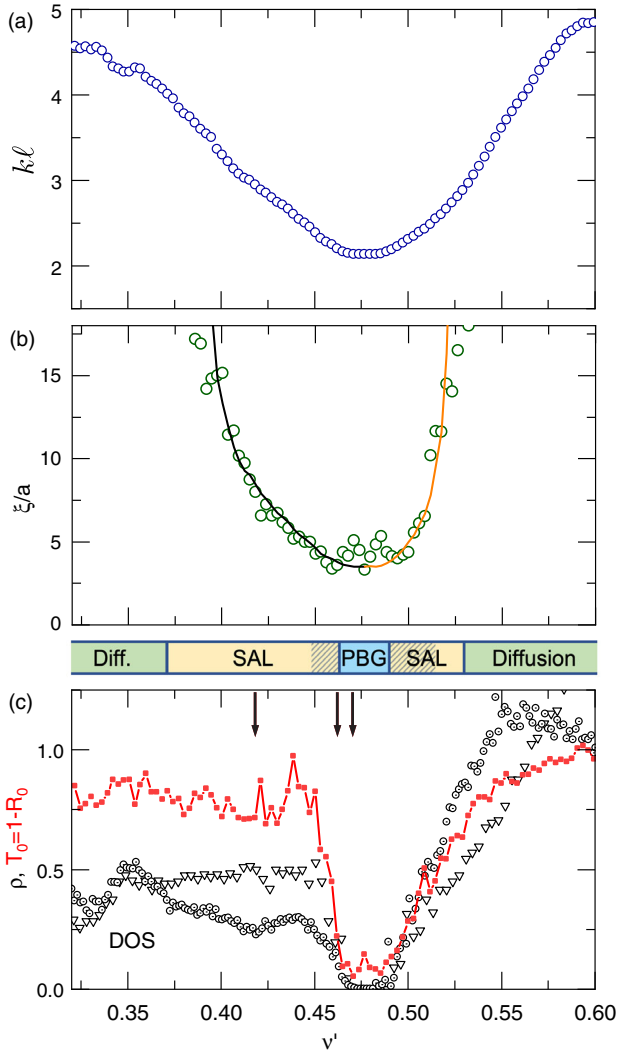

FIG. 4. Frequency dependence of the transport parameters determined from the fit to the FDTD data $T(L)$, as described in Fig. 3. (a) Reduced mean free path $k\ell = 2\pi\ell/\lambda = 2\pi\nu'\ell/a$. (b) Localization length ξ/a. Lines show the scaling prediction from SC theory, $\xi/a \propto (k\ell)^2/\{1-[k\ell/(k\ell)_c]^4\}$, with $(k\ell)_{c,l} \simeq 4.1$ (black line) and $(k\ell)_{c,h} \simeq 2.85$ (orange line) and a prefactor of order 1. The different transport regimes are indicated at the bottom. (c) Red solid squares: $T_0 = 1 - R_0$, compared to numerical calculations of the DOS ρ (open symbols). The DOS data has been reproduced from Ref. [6] (circles) and Ref. [15] (triangles). The arrows indicate the frequencies for the data shown in Fig. 3.

in the nominator: $\xi/\ell^* \propto (1/(3/\pi - \rho(k\ell^*)^2))$. This expression agrees well with our data for ξ/ℓ if we, again, use $\ell^* = \ell$ and replace $k\ell$ by $k\ell/(k\ell)_c$ [36], as shown in the Supplemental Material [30], Fig. S2. Note that the influence of the density of states on ξ is small since $\rho < 1$ only in a regime where $k\ell/(k\ell)_c \ll 1$.

Density of states and coherent reflection.—It seems plausible that the normalized DOS is responsible for the observed direct reflection since, for a full bandgap, we know that the DOS is zero and $R_0 \equiv 1$. Here, we consider the DOS normalized by the density of states of the "homogeneous" medium [6,15]. In and near the bandgap, the coherent beam's intensity and the z dependent local DOS (LDOS) decay exponentially to their bulk values over a distance of a mean free path $\ell \ll \xi$. In the bulk, the mean LDOS is equal to bulk DOS $\rho(\nu')$, and thus, for $L \gg \ell$, we expect $T_0(\nu') \simeq \rho(\nu')$. Hasan *et al.*, as well as Skipetrov, argued similarly when discussing finite-sized effects in photonic crystals where the incident beam's coherent intensity $T(z) = 1 - R(z)$ and the LDOS decay exponentially. For a crystal, the decay length is the Bragg length L_B [39–41]. Koenderink *et al.* discussed the attenuation of the coherent beam for the case of disorder in photonic crystals [42].

In Fig. 4(c), we compare $T_0(\nu')$ values from the fit with direct calculations of the DOS. The DOS data were previously published by Hui Cao and coworkers [6] and by us [15,34] for the same or very similar structures.

Origins of the bandgap.—Some remarks concerning the origins of the bandgap are in order. This Letter shows that resonant scattering in the presence of correlated disorder leads to destructive interference in the forward direction and enhanced single scattering reflection. Backscattering can also be induced by single scattering resonances [43]. This microscopic picture of preferential backscattering is supported, at least up to the lowest order, by recent diagrammatic calculations [44]. Zhang-Stillinger and Torquato argued that another structural property is essential for forming a bandgap. Uniformity and resulting bounded hole sizes (empty regions) prevent deep penetration of unscattered photons into the bulk of the material [45,46]. They say that such structural "rigidity" confers novel physical properties to disordered systems, including the desired bandgap. Qualitatively, stealthy hyperuniformity can provide both mechanisms. Stealthiness implies bounded hole sizes [45] and suppresses scattering at scattering angles $\vartheta < \vartheta_c$ [$q_\vartheta = 2k\sin(\vartheta/2) < q_c$] through collective scattering and destructive interference [11,23]. For a quantitative microscopic assessment, however, higher-order scattering loops, beyond the collective scattering approximation, must be taken into account [44].

Summary and conclusion—In this Letter, we study the transmission of light through hyperuniform, high refractive index networks using numerical simulations and theory. We propose adding a direct reflection term to the theoretical model describing light transmission through optically dense amorphous photonic materials. Combined with the results of the self-consistent theory of localization for a semi-infinite medium, we derive a simple, closed-form analytical expression for the total transmission coefficient of optically dense slabs $T_d(L)$ [16–18]. Our model captures the optical transmission behavior between localization and the bandgap. Moreover, we rationalize that near and inside the gap, the reduced density of states is responsible for the coherent reflection and the attenuation of the coupling of

the incident light beam to diffuse and localized transport. The quantitative agreement of our theory with numerical simulations suggests that it could be of considerable value for experimental studies. Moreover, this study shows that, for an amorphous PBG material in the gap, the scattering mean free path ℓ is equivalent to the Bragg length in a photonic crystal [1,47]. This observation is essential, and the behavior is different from disordered photonic crystals, where the Bragg length is given by the periodically repeating environment and the scattering length by the degree of disorder [41,42,48,49].

We thank Sergey Skipetrov and Arthur Goetschy for insightful discussions. The Swiss National Science Foundation supported this work through the National Centre of Competence in Research "Bio-Inspired Materials," Grant No. 182881 (F. S. and L. F. P.), Projects No. 149867 (F. S.) and No. 197146 (L. F. P.).

*frank.scheffold@unifr.ch

[1] J. D. Joannopoulos, S. G. Johnson, J. N. Winn, and R. D. Meade, *Photonic Crystals: Molding the Flow of Light* (Princeton University Press, Princeton, NJ, 2008).
[2] A. Lagendijk, B. Van Tiggelen, and D. S. Wiersma, Phys. Today **62**, No. 8, 24 (2009).
[3] E. Yablonovitch, Phys. Rev. Lett. **58**, 2059 (1987).
[4] K. Edagawa, S. Kanoko, and M. Notomi, Phys. Rev. Lett. **100**, 013901 (2008).
[5] M. Florescu, S. Torquato, and P. J. Steinhardt, Proc. Natl. Acad. Sci. U.S.A. **106**, 20658 (2009).
[6] S. F. Liew, J.-K. Yang, H. Noh, C. F. Schreck, E. R. Dufresne, C. S. O'Hern, and H. Cao, Phys. Rev. A **84**, 063818 (2011).
[7] N. Muller, J. Haberko, C. Marichy, and F. Scheffold, Adv. Opt. Mater. **2**, 104 (2014).
[8] W. Man, M. Florescu, E. P. Williamson, Y. He, S. R. Hashemizad, B. Y. C. Leung, D. R. Liner, S. Torquato, P. M. Chaikin, and P. J. Steinhardt, Proc. Natl. Acad. Sci. U.S.A. **110**, 15886 (2013).
[9] S. R. Sellers, W. Man, S. Sahba, and M. Florescu, Nat. Commun. **8**, 14439 (2017).
[10] L. S. Froufe-Pérez, M. Engel, P. F. Damasceno, N. Muller, J. Haberko, S. C. Glotzer, and F. Scheffold, Phys. Rev. Lett. **117**, 053902 (2016).
[11] S. Torquato, G. Zhang, and F. H. Stillinger, Phys. Rev. X **5**, 021020 (2015).
[12] L. S. Froufe-Pérez, M. Engel, J. J. Sáenz, and F. Scheffold, Proc. Natl. Acad. Sci. U.S.A. **114**, 9570 (2017).
[13] G. J. Aubry, L. S. Froufe-Pérez, U. Kuhl, O. Legrand, F. Scheffold, and F. Mortessagne, Phys. Rev. Lett. **125**, 127402 (2020).
[14] F. Sgrignuoli, S. Torquato, and L. Dal Negro, Phys. Rev. B **105**, 064204 (2022).
[15] J. Haberko, L. S. Froufe-Pérez, and F. Scheffold, Nat. Commun. **11**, 4867 (2020).
[16] P. Wölfle and D. Vollhardt, Int. J. Mod. Phys. B **24**, 1526 (2010).
[17] N. Cherroret, S. E. Skipetrov, and B. A. van Tiggelen, Phys. Rev. E **82**, 056603 (2010).
[18] B. A. van Tiggelen, A. Lagendijk, and D. S. Wiersma, Phys. Rev. Lett. **84**, 4333 (2000).
[19] D. Durian, Physica (Amsterdam) **229A**, 218 (1996).
[20] P.-A. Lemieux, M. U. Vera, and D. J. Durian, Phys. Rev. E **57**, 4498 (1998).
[21] A. Ishimaru, *Wave Propagation and Scattering in Random Media* (Academic Press, New York, 1978), Vol. 2.
[22] P. Kaplan, M. H. Kao, A. Yodh, and D. J. Pine, Appl. Opt. **32**, 3828 (1993).
[23] O. Leseur, R. Pierrat, and R. Carminati, Optica **3**, 763 (2016).
[24] S. M. Graves and T. G. Mason, J. Phys. Chem. C **112**, 12669 (2008).
[25] N. Cherroret and S. E. Skipetrov, Phys. Rev. E **77**, 046608 (2008).
[26] R. Carminati and J. C. Schotland, *Principles of Scattering and Transport of Light* (Cambridge University Press, Cambridge, England, 2021).
[27] S. Magkiriadou, J.-G. Park, Y.-S. Kim, and V. N. Manoharan, Phys. Rev. E **90**, 062302 (2014).
[28] V. Hwang, A. B. Stephenson, S. Magkiriadou, J.-G. Park, and V. N. Manoharan, Phys. Rev. E **101**, 012614 (2020).
[29] Z. Wang, C. L. C. Chan, T. H. Zhao, R. M. Parker, and S. Vignolini, Adv. Opt. Mater. **9**, 2100519 (2021).
[30] See Supplemental Material at http://link.aps.org/supplemental/10.1103/PhysRevLett.129.157402 for additional data and plots, an approximate expression for $T(L)$ covering the whole range of L, and a comparison to a recently published formula for the localisation length.
[31] A. F. Oskooi, D. Roundy, M. Ibanescu, P. Bermel, J. D. Joannopoulos, and S. G. Johnson, Comput. Phys. Commun. **181**, 687 (2010).
[32] C. Song, P. Wang, and H. A. Makse, Nature (London) **453**, 629 (2008).
[33] A. Ikeda and L. Berthier, Phys. Rev. E **92**, 012309 (2015).
[34] J. Haberko, L. S. Froufe-Prez, and F. Scheffold, Transition from light diffusion to localization in three-dimensional amorphous dielectric networks near the band edge, data repository Zenodo, 10.5281/zenodo.3968424 (2020).
[35] L. Cobus, W. Hildebrand, S. Skipetrov, B. Van Tiggelen, and J. Page, Phys. Rev. B **98**, 214201 (2018).
[36] S. Skipetrov and I. Sokolov, Phys. Rev. B **98**, 064207 (2018).
[37] R. Monsarrat, Propagation of light waves in correlated disordered media: Density of states, transport, localisation, Ph.D. thesis, Université de Paris, Institut Langevin, ESPCI Paris—PSL, CNRS, 2022, https://hal.archives-ouvertes.fr/tel-03765743.
[38] J. Haberko and F. Scheffold, Opt. Express **21**, 1057 (2013).
[39] S. B. Hasan, A. P. Mosk, W. L. Vos, and A. Lagendijk, Phys. Rev. Lett. **120**, 237402 (2018).
[40] S. E. Skipetrov, Eur. Phys. J. B **93**, 70 (2020).
[41] P. D. García, R. Sapienza, C. Toninelli, C. López, and D. S. Wiersma, Phys. Rev. A **84**, 023813 (2011).
[42] A. F. Koenderink, M. Megens, G. Van Soest, W. L. Vos, and A. Lagendijk, Phys. Lett. A **268**, 104 (2000).

[43] R. Gómez-Medina, L. S. Froufe-Pérez, M. Yépez, F. Scheffold, M. Nieto-Vesperinas, and J. J. Sáenz, Phys. Rev. A **85**, 035802 (2012).
[44] R. Monsarrat, R. Pierrat, A. Tourin, and A. Goetschy, arXiv:2110.12034.
[45] G. Zhang, F. H. Stillinger, and S. Torquato, Soft Matter **13**, 6197 (2017).
[46] S. Ghosh and J. L. Lebowitz, Commun. Math. Phys. **363**, 97 (2018).
[47] P. D. García, R. Sapienza, L. S. Froufe-Pérez, and C. López, Phys. Rev. B **79**, 241109(R) (2009).
[48] C. Conti and A. Fratalocchi, Nat. Phys. **4**, 794 (2008).
[49] S. Aeby, G. J. Aubry, N. Muller, and F. Scheffold, Adv. Opt. Mater. **9**, 2001699 (2021).